Sensitivities in rock mass properties

A DEM insight

Cédric Lambert* — John Read**

** Department of Civil and Natural Resources Engineering,*
University of Canterbury
Private Bag 4800, Christchurch 8140, New Zealand
cedric.lambert@canterbury.ac.nz

*** CSIRO, Earth Science and Resource Engineering*
Queensland Centre for Advanced Technologies
PO Box 883, Kenmore QLD 4069, Australia

ABSTRACT. *This work proposes to look at the variation of some engineering properties of a rock mass (strength and stiffness) with respect to some structural and mechanical properties. Based on standard laboratories properties and field measurements, a discrete element model of a particular rock mass has been generated using the Synthetic Rock Mass approach (SRM). Large scale specimens are generated combining DEM to represent the rock and 3D discrete fracture network models to represent the structure pattern. The specimens of rock mass are then numerically tested. Series of compression tests have been performed on different samples varying loading direction, sample size, intact rock strength, joint size and joint spacing. Results of the simulations are presented here and sensitivity of the rock mass mechanical properties to these parameters is discussed.*

RÉSUMÉ. *Ce travail propose d'étudier la variation de propriétés mécaniques d'un massif rocheux avec certaines caractéristiques géologiques et mécaniques. Une approche dite « Synthetic Rock Mass » (SRM) a été utilisée pour développer un modèle éléments discrets du massif rocheux. Ces modèles SRM sont élaborés sur la base de propriétés mesurées in situ ou en laboratoire. Cette méthode permet de construire et de tester numériquement des échantillons de roche de grande échelle pour lesquels la fracturation naturelle du massif est introduite. Plusieurs séries d'essais numériques de compression simple ont ainsi été réalisées pour différentes valeurs de la résistance à la compression simple de la roche intacte, différents tailles et espacements des discontinuités. Les résultats de ces essais sont présentés et la sensibilité des propriétés mécaniques du massif rocheux discutée.*

KEY WORDS: *DEM, jointed rock mass, anisotropy, scale effects*

MOTS-CLÉS: *MED, massifs rocheux fracturés, anisotropie, effets d'échelle*

1. Introduction

A fundamental characteristic of jointed rock mass is the presence of structural defects. These geological structures vary in nature (joints, faults, bedding planes) and in scale (from centimetres to hundreds of meters). Being a key component of rock masses, they affect the geomechanical behaviour of jointed rock. Extrapolating field measurements and laboratory testing results to geotechnical properties of jointed rock mass is a challenging exercise and practitioners usually refer to empirical classification systems (e.g. RMR, GSI). The recent development of the synthetic rock mass approach (SRM) and other equivalent is offering new perspectives in our understanding of rock mass behaviour. The SRM approach is a methodology that has been developed by Pierce et al. (2007) within PFC3D in order to predict the mechanical behaviour of jointed rock masses. The methodology involves the construction and testing of a 3D SRM sample. SRM samples represent the rock mass as an assembly of bonded particles where a joint network is introduced as a series of disc-shaped fractures. The methodology describes the joints behaviour using a smooth joint model. This approach brings together the benefits of two methods, the bonded particle model proposed by Potyondy and Cundall (2004) to simulate intact rock and DFN simulations to construct a 3D joint pattern (Rogers et al., 2009; Elmouttie et al., 2010). Many different loading paths can then be applied to SRM samples of different shapes to predict the behaviour of the rock mass. Using only data obtained from standard rock mass characterisation methods, the methodology has proven its ability to reproduce a wide range of typical behaviours of a rock mass. For a detailed description of the methodology one can refer to Pierce et al. (2007) or Mas Ivars et al. (2008). In the present work, the SRM methodology has been used to study the rock mass mechanical properties in a complex geological environment. The models have been developed using real mine data, coming from an open pit mine in Western Australia. A particular emphasis has been made on one geotechnical domain, namely 1900S1. Sensitivities of the mechanical properties of the SRM models are presented and effects of lithology, joint size and fracture frequency are discussed.

2. Development of the Discrete Fracture Network model

2.1. Discrete fracture network generation

Discrete Fracture Network (DFN) modelling provides powerful means of representing fracture systems based on available structural data. These stochastic approaches aim at generating representative models of the structural conditions, observed in the field, accounting for structural data coming borehole, scan lines or window mapping. Structural information from one geotechnical domain, namely 1900S1, has been used to develop a DFN using JointStats, a discontinuity data management system developed at the University of Queensland (JKMRC, 2000).

Joints are assumed to be circular discs distributed according to a Poisson process. The persistence of joints is estimated from trace length information. Once a shape for the size distribution has been chosen (log normal, exponential or beta distribution), the parameters of the distribution are fitted using the maximum likelihood theory (Lyman, 2003). To ensure that the fracture frequencies are also in agreement with the logged data, JointStats returns a value of the density of the joints in space (number of joint centres per cubic meter). In broad terms, the observed shapes of the trace length distributions on the various scan lines will determine the persistence parameters and the numbers of traces will control the value of the joint density.

A total of five joint sets have been defined as illustrated on Figure 1. Subvertical jointing is clearly predominant, with a preferred orientation striking roughly North-South. However a strong subhorizontal joint set can be identified. The fracture generation process resulted in the fracture characteristics given in ***Table 1***. The resulting three dimensional fractrure network, 200m x 200m x 200m volume, is illustrated in Figure 1. The current DFN realisation contains 35,011 joints.

Table 1. *Fracture characteristics of the generated fracture system*

Fracture characteristics	Set 1	Set 2	Set 3	Set 4	Set 5
Dip [°]	75.6	76.70	6.60	70.80	79.90
Dip direction [°]	261.9	96.90	14.20	356.0	135.70
Fracture intensity P_{32} [m^{-1}]	0.461	0.152	0.357	0.073	0.033
Mean diameter [m]	7.48	13.37	14.99	4.43	14.72

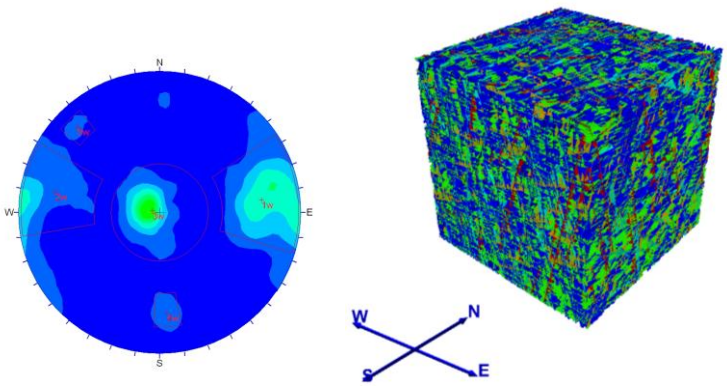

Figure 1. *Stereonet representation of structures in domain 1900S1 (left) and visualisation of the generated 200m wide Discrete Fracture Network (right)*

The joints will be represented as planar surfaces with the newly developed smooth joint contact model (Itasca, 2008). In this new contact scheme, a sliding plane is introduced through a dip and dip direction for each contact between particles that lie upon opposite sides of the specified plane. This plane defines the general direction of sliding of the particles which are set free to overlap each-other. This new formulation has proven its ability to capture the behaviour of jointed rock masses (Pierce et al., 2007; Deisman et al., 2010; Esmaieli et al., 2010) and the behaviour of rock joints (Lambert and Coll, 2010). Joints have been considered to be purely frictional (no cohesion) with a friction angle of 30°. Normal and shear stiffness have been set to 150e9 Pa/m and 20e9 Pa/m respectively. No dilation has been introduced in the description. The same mechanical properties were assigned to all fractures.

3. Development of an equivalent rock mass model

The general workflow of the Synthetic Rock Mass approach consists of generating a Discrete Fracture Network (DFN) model incorporating all the joint attributes (e.g. spacing, trace length and orientation). The DFN closely represents the true rock mass fabric/structure. The intact rock blocks/bridges between the structures (e.g. joints) are represented as an assembly of spherical bonded particles. Large rock mass samples are hence numerically constructed and tested under many loading conditions (confining stress, loading directions, sample size). The results provide directional constitutive behaviour at different scales, which can then be used for more conventional engineering analysis.

3.1. Properties

Intact rock has been modelled as a bonded particle assembly using PFC3D. Microproperties have been calibrated for each rock type against laboratory test results using standard sample generation and testing procedures (Potyondy and Cundall, 2004). The DFN presented in section 2 unveils a maximum fracture frequency, or joint frequency, of 0.61 in an East-West direction (0.18 North-South and 0.54 vertically). The maximum fracture frequency relates to the typical minimum size of a rock bridge in the rock mass (i.e. average size of pieces of intact rock). The E-W direction exhibits the smallest average rock bridge size, 1.64m. Numerical specimens of a similar size are used for the calibration of microproperties. Behaviour of rock bridges will hence match the behaviour of intact rock, estimated through standard laboratory testing. 2m x 2m x 4m core specimen have been used for the calibration with a minimum particle radius of 0.2m and a maximum to minimum ratio of 1.66 resulting in a particle resolution (i.e. number of particle across the width of the sample) of 4. For each rock type microproperties have been adjusted until a reasonable match between the behaviour of the particle assembly and the target properties, as given in Table 2.

In some complex geological environments, mapping the distribution of each rock type in detail is inefficient to impossible because of the sparse distribution of exploration data. However it has been possible to characterise the statistical distribution of rock types in the domain from available boreholes. In the present study, the geotechnical domain 1900S1 consists predominantly of three rock types, 56% of mafic volcanics, 24% of mafic intrusive and 20% of basalt. In order to represent the rock composition of the geotechnical domain, a model of intact rock containing all three rock types in the same proportion has been generated with rock types randomly distributed. Properties of the mutli rock model are given in Table 2. In reality, the rock units may well be distributed in lensoidal shapes or laminated and creation of a randomly distributed mixture of the rock types is only first approach to consider the variety of rocks in the analysis.

Table 2. Measured (lab.) and simulated (PFC3D) intact rock properties

	UCS [MPa]		Young's Modulus [GPa]	
	Lab.	PFC3D	Lab.	PFC3D
Mafic intrusive	113.7	107.9	96.6	98.0
Mafic volcanic	74.3	70	28.8	29.5
Basalt	170	166.3	30	30
Multi rock		112.6		70.9

3.2. Constitutive behaviour of the rock mass

Two industry standard tests have been simulated to provide measures of compressive strength at various confining pressures σ_3 and secant elastic moduli of the rock mass (E_{rm}), taken at 50% of the peak stress. These tests have been performed for three different loading directions (x, y, z), corresponding to East-West, North-South, and vertical directions to quantify any geomechanical anisotropy. Samples of three different sizes have been tested (24m side, 12m side and 6m side) to investigate the scale dependency of the geomechanical properties of the rock mass. Rock mass properties being variable three 24m wide rock mass samples have been tested as well as nine 12m wide and nine 6m specimens.

3.2.1.Uniaxial compression test result

A series of uniaxial compressive tests were performed on all 21 rock mass samples. In order to speed up the testing of these large samples a procedure using particle as boundaries has been used (Itasca, 2008). Grip spheres at the top and bottom of each sample are identified as plates and loading is performed using the internal based method which assigns linearly varying axial velocities to all assembly particles (Pierce et al., 2007; Esmaieli et al., 2010). One test took approximately 30h to run on a 32 bit Intel quad core 3GHz processor computer.

24m rock mass specimens can be seen in Figure 2. The distinct levels of shading correspond to contiguous blocks, within which any particles can be reached from any other via one or more intact bonds. Between such blocks there are unbounded contacts. Between such blocks, there unbounded contacts associated with joint segments. During loading, samples become more fragmented as bonds break. Although a block is identified with uniform shading, it may contain many dead-end fractures, or partially through going, that may extend during loading.

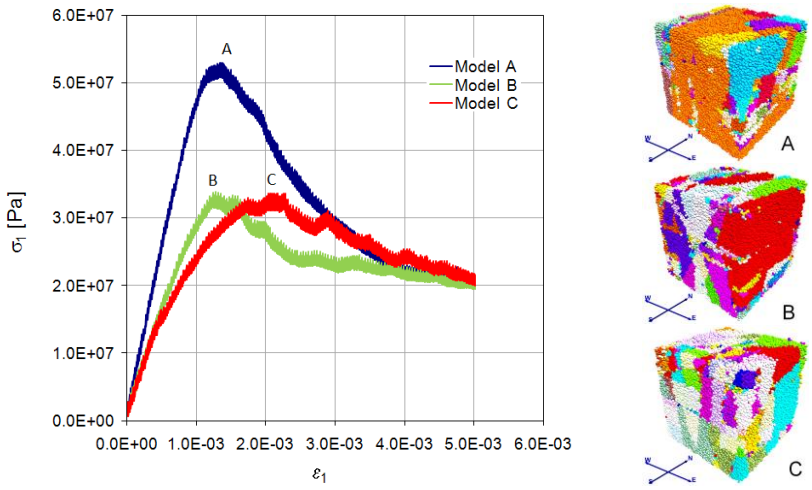

Figure 2. *Stress-strain plots during unconfined compression tests and visualisation of 24m wide SRM specimens.*

Figure 2 shows the stress strain plots for three 24m wide rock mass samples. The fracture patterns were taken from different locations of the same DFN realisation and are referred to as A, B and C. The models exhibited a fracture intensity ranging from 1.96 m^{-1} to 2.37 m^{-1} and a number of individual blocks ranging from 548 to 927. Samples B and C show a similar peak strength, 31.6 MPa and 31.1 MPa respectively, and a similar secant Young's modulus, 31 GPa and 26.7 GPa respectively. Sample A exhibited higher peak strength, 53 MPa, and higher secant Young's modulus, 50 GPa. This variability can be attributed to the initial degree of fracturation of the models as number of blocks and fracture intensity were significantly lower for sample A.

3.2.2.Anisotropy

The strength of a rock mass cannot be defined only through its UCS. The SRM samples have been submitted to a series of numerical triaxial compression tests at various confining pressures (0, 2 and 10 MPa) from which a partial strength

envelope is obtained. The average strength of the 24m wide specimens tested in East-West loading direction, North-South and vertical are summarized in Figure 3. A clear anisotropy is enhanced in the horizontal plane between N-S and E-W directions and with the vertical direction. The rock mass appears stronger in an E-W direction whereas loading in a N-S direction is the most unfavourable of the tested directions. The observed anisotropy is in agreement with the overall joint fabric of the rock mass. The DFN consists of three predominant joint sets (namely 1, 2 and 3 in ***Table 1***). Sets 1 and 2 are nearly orthogonal to the E-W direction, hence showing limited impact on strength in that direction. Similarly Set 3 is nearly horizontal and will primarily affect loading in horizontal directions.

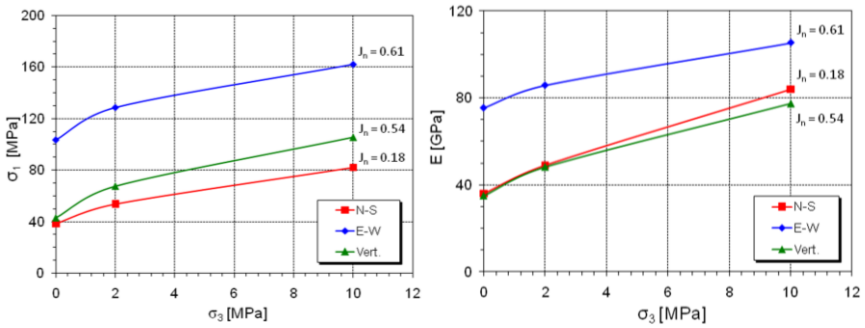

(a) (b)

Figure 3. *Average results of triaxial compression tests for three loading directions: N-S (square), E-W (diamond) and vertical (triangle). (a) Peak stress versus confining stress σ_3 and (b) Young's modulus E_r, versus σ_3.*

Similar observations can be made on the elastic modulus E_{rm}., for which higher values are obtained in E-W direction. Interestingly, little difference is observed between N-S and vertical directions, vertical even being lower at high confining pressure. The overall anisotropy appears to be reduced as confining pressure σ_3 increases.

3.2.3.Scale

Nine 12m side cubic specimens and nine 6m side cubic specimens have been tested under unconfined compression in a N-S loading direction. Results of numerical tests are summarized in Figure 4 for which both average values and range of variation for peak shear strength and rock mass deformation modulus E_{rm} are plotted. Average peak strength decrease with sample width from 112.6 MPa for intact rock to 38.6 MPa for 24m wide specimens whereas average elastic modulus decreases from 70.9 GPa to . It can be observed that variation decreases as sample

size increases. Similar trends have been observed by Cundall et al. (2008) and Esmaieli et al. (2010).

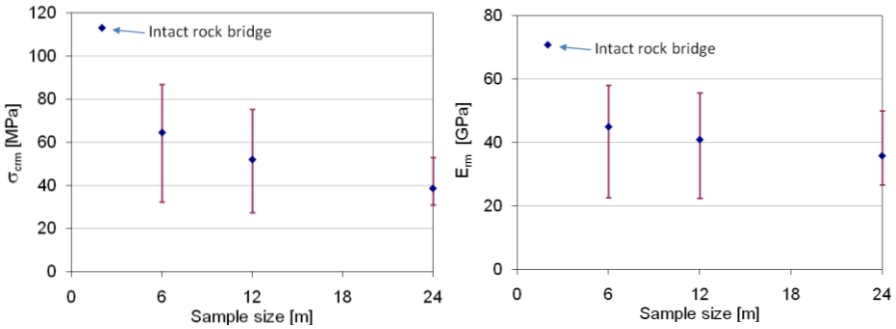

(a) (b)

Figure 4. *Size effect on unconfined compressive strength of the rock mass σ_{crm} and elastic modulus E_{rm}*

4. Sensitivity analyses of rock mass properties

4.1. Sensitivity to lithology

In the current practice, rock mass strength is usually characterised by its unconfined compressive strength, namely σ_{crm}. Since the 1900S1 domain is represented by a random distribution of three different rock units, three independent UCS tests were conducted to study the impact of individual rock strength in the strength of the fractured rock mass. Three homogeneous rock mass specimens have generated for each lithology with joint patterns A, B and C: three mafic volcanic rock masses, three mafic intrusive rock masses and three basalt rock masses. The nine specimens have been submitted to UCS compression tests in the North-South direction which results are presented in Figure 4 alongside measured rock mass elastic moduli E_{rm}.

For each individual structure patterns, represented by model A, B and C, the uniaxial compressive strength of the synthetic rock mass, σ_{crm}, exhibits a linear variation with intact rock strength, σ_{ci}. Similarly rock mass elastic modulus, E_{rm}, varies linearly with intact rock Young's modulus, E_i. Correlations using average values for σ_{crm} and E_{rm} are given in Figure 5. The coefficients of proportionality α_n and β_n reflect the structures forming the rock fabric of the specimen. They can be expected to be a function of joint orientation, size, density and scale of the specimen. The mechanical properties of the fractures will certainly be of major importance.

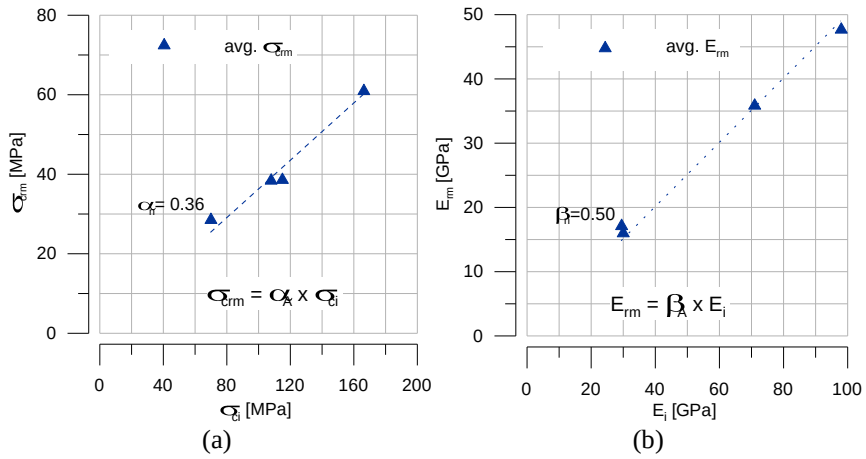

Figure 5. *Variation of average rock mass properties with different lithologies: (a) σ_{crm} versus σ_{ci} and (b) E_{rm} versus E_i*

4.2. Sensitivity to structural properties

4.2.1.Joint size

In order to study sensitivity of rock mass properties to the size of its discontinuities, seven 24m SRM samples have been created using seven different joint patterns. For each of them, the intact rock component has been considered to be a mixture of the three individual rock types as defined in section 3. The structural pattern corresponding to model B has been used as the reference rock fabric. Six additional structural patterns have been obtained multiplying the diameter of each joint of the reference fabric by a constant factor s (0.5, 0.7, 0.9, 1.1, 1.2 and 1.5). As s increases, the persistence of joints increases. The newly created fabrics have then been added on top of the bonded particle assembly, hence generating seven new SRM specimens, the only difference between each SRM samples being the joint size. Each SRM has the same number of joints and each joint has exactly the same position and the same orientation. The specimens cover a wide range of interlocking of rock pieces, from massive rock mass for s=0.5 to very blocky for s=1.5 (Figure 6). For s=0.5, three blocks represent 96% of the total volume of the rock mass specimen. For the reference sample (s=1.0), two individual block forms 58% of its volume and for s=1.5, the block sizes are more evenly distributed.

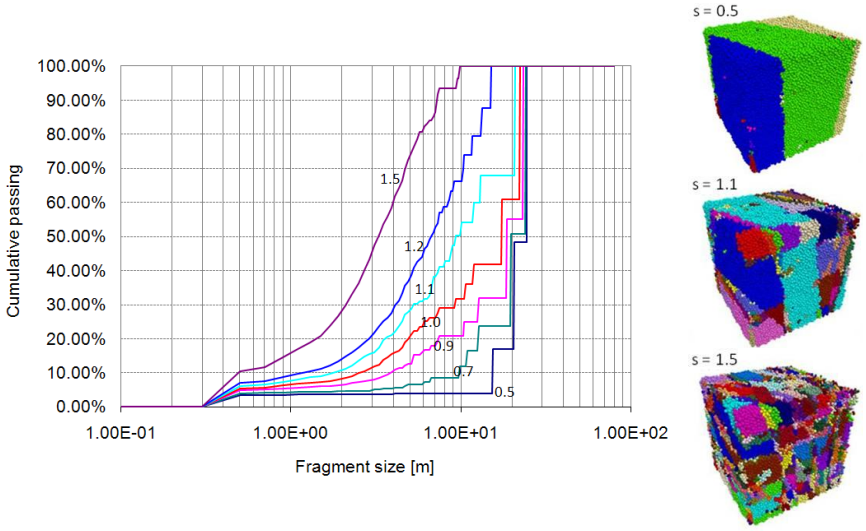

Figure 6. *Fragmentation curves of rock mass specimens with different joint size multiplicative factor s*

Results of UCS tests performed in the N-S direction are reported on Figure 7. The case of intact rock, corresponding to s=0, has also been reported, σ_{ci} = 112.6 MPa. The relation appears to be bilinear in that case and two linear best fits have been obtained, for $s \leq 1.1$ and for $s \geq 1.1$. Best fit equations are given in Figure 7. This suggests that the strength reduction is driven by two distinct phenomena. The fragmentation curves in Figure 6 inform on the size distribution of the continuous block within the sample. In a continuous block, the particles are linked together with a continuous chain of bonds. Those blocks can have partial cracks or embedded cracks but form one single piece of rock. Figure 6 shows that for a multiplicative factor s lower than 1.1, more than 30% of the rock mass volume is continuous. For a multiplicative factor of 1.2 and above the rock mass appears clearly more and more discontinuous. In the first case, one can expect the loading to be mostly carried by this large individual piece of rock. The strength of the rock will thus be directly linked to the strength of that particular block and more specifically to the strength of the rock bridges in that block. Failure requires brittle fractures through intact rock to occur. Increasing the size of the joints reduces the size the rock bridges, hence weakening the SRM sample. In the second case, the SRM sample is more discontinuous. With the joint persistence increasing, the rock mass is evolving towards a blocky rock mass. The behaviour of the rock mass is mainly controlled by the interlocking of the blocks.

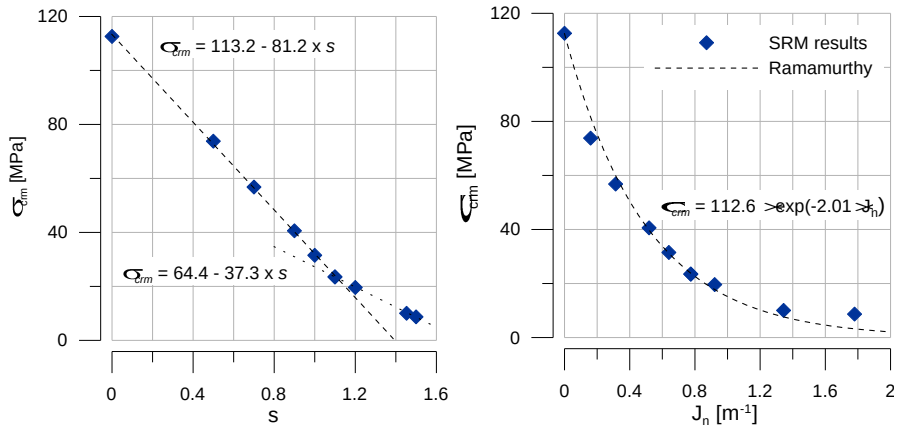

Figure 7. *Evolution of unconfined compressive strength of the rock mass σ_{crm} with joint size: (a) σ_{crm} as a function of joint size multiplicative factor s. (b) σ_{crm} as a function of the fracture frequency in the loading direction J_n*

4.2.2.Effect of fracture frequency

Ramamurthy (2001) proposed a formulation where the strength of a rock mass was expressed as function of a joint factor J_f. The joint factor is function of the joint frequency in the loading direction J_n, of a coefficient n reflecting the inclination of the joint and of the friction coefficient r. This formulation was established compiling the results of various experimental studies from the literature where the compressive strength of jointed rock samples was analysed. Different rock types and all sorts of fracture patterns were used. All those results could be described using one single formulation through the joint factor.

$$\sigma_{crm} / \sigma_{ci} = \exp\left(-\alpha \cdot J_f\right) \quad \text{with } J_f = J_n / (r \cdot n) \qquad [1]$$

Where σ_{crm} is the jointed rock compression strength, σ_{ci} is the intact rock compression strength and α a positive constant number.

The effects of the various modifications on the fracture networks, joint size modifications presented in section 4.2.1 can been compiled in terms of fracture frequency, J_n. For each 24m specimen, the fracture frequency in the loading direction (i.e. N-S) has been estimated. The rock mass strengths are then plotted versus the fracture frequency of the corresponding joint pattern on Figure 7. A negative exponential formulation can be fitted to describe the decrease of the SRM strength with the fracture frequency J_n. The best fit is given by the following, with a coefficient of determination R^2 of 0.988:

$$\sigma_{crm} = 112.6 \exp\left(-2.01 \cdot J_n\right) \quad [2]$$

Where 112.6 corresponds to the compressive strength of the intact mixture σ_{ci} and J_n represents the joint fracture frequency in the North-South direction. The results obtained with the SRM exhibit a qualitative match with Ramamurthy's formulation. However a significant difference persists regarding the exponential constant (2.01 for the SRM and between 0.004 and 0.01 for Ramamurthy, 2001). This difference cannot be explained only by the introduction of the coefficient n and the friction r in the joint factor definition and requires further investigation.

5. Conclusions

The development of the SRM methodology and equivalents has been a step forwards for the characterisation of the constitutive behaviour of a rock mass. In this study, the SRM approach has been applied to complex mining environment where it is not possible to divide geotechnical domains with respect to lithology. An alternative approach has been developed combining the different rock types on the basis of their relative proportion observed in the field. Typical behaviour of jointed rock masses have been observed including fractures induced anisotropy, scale dependence. The observed anisotropy in the constitutive behaviour of the SRM samples was in agreement with the orientation of the joint sets introduced in the model.

Sensitivity analyses have been performed on the mechanical properties of the synthetic rock mass. Influences of lithology, joint size, spacing and frequency have been investigated. Simulations have enhanced a strong linear relationship between unconfined compression strengths of the rock mass σ_{crm} and of its intact rock. Similarly Young's modulus of the rock mass has been observed to vary linearly with Young's modulus of intact rock. Another aspect that has been investigated is the effect on rock mass behaviour of some parameters of the fracture network. SRM samples varying joint size have been generated and tested. As expected the strength of the rock mass decreased as joint size increased. The results show a bilinear relation suggesting the decrease having two distinct sources. For small joints, failure required brittle failure through rock bridges. Strength decrease was hence attributed to the size reduction of rock bridges. For larger joints, the rock mass could be described as blocky, limited brittle fracturing was required. Strength was attributed mainly to interlocking. The relation between rock mass strength and joint frequency could be described with a negative exponential, showing a qualitative agreement with experimental data from the literature.

6. References

Cundall P.A., Pierce M.E., Mas Ivars D. « Quantifying the Size Effect of Rock Mass Strength », in *Proc. 1st Southern Hemisphere International Rock Mechanics Symposium*, Perth, 2008, p 3-15.

Deisman N., Mas Ivars D., Darcel C., Chalaturnyk R.J., « Empirical and numerical approaches for geomechanical characterization of coal seam reservoirs », *International Journal of Coal Geology*, 82, 2010, p. 2204-212.

Elmouttie M., Poropat G., Krähenbühl G., « Polyhedral modelling of underground excavations », *Computers and Geotechnics*, 37, 2010, p. 529-535

Esmaieli K, Hadjigeorgiou J. and Grenon M. « Estimating geometrical and mechanical REV based on synthetic rock mass models at Brunswick Mine », *International Journal of Rock Mechanics & Mining Sciences*, 47, 2010, p 915-920.

Itasca Consulting Group Inc., Particle Flow Code in 3 Dimensions, Version 4.0, 2008.

JKMRC, JoinStats, Version 1.15, 2000.

Lambert C., Coll C., « A DEM approach to rock joint strength estimates », in *Rock Slope Stability in Open Pit Mining and Civil Engineering*, Santiago,2009.

Lyman G.J., « Rock fracture mean trace length estimation and confidence interval calculation using maximum likelihood methods », *International Journal of Rock Mechanics & Mining Sciences*, 40(6), 2003, p. 825–832.

Mas Ivars D., Pierce M., DeGagnné D., Darcel C., « Anisotropy and scale dependency in jointed rock-mass strength – A Synthetic Rock Mass Study », in *Proceedings First International FLAC/DEM Symposium on Numerical Modeling*, Minneapolis, USA, 2008.

Pierce M., Cundall P., Potyondy D. and Mas Ivars D., « A Synthetic Rock Mass Model for Jointed Rock », in *Rock Mechanics: Meeting Society's Challenges and Demands*, *1st Canada–US Rock Mechanics Symposium*, Vancouver, 2007, p. 341–349.

Potyondy D.O., Cundall, P.A. (2004) « A Bonded-Particle Model for Rock », *International Journal of Rock Mechanics & Mining Sciences*, 41(8), pp. 1329–1364.

Ramamurthy, T., « Shear strength response of some geological materials in triaxial compression », *International Journal of Rock Mechanics & Mining Sciences*, 38(5), 2001, p. 683–697.

Rogers S., Elmo D., Beddoes R., Dershowitz W., « Mine scale DFN modelling and rapid upscaling in geomechanical simulations of large open pits », in *Proc. Rock Slope Stability in Open Pit Mining and Civil Engineering*, Stantiago, 2009.